Journal of Statistical Mechanics: Theory and Experiment
An IOP and SISSA journal

PAPER: Disordered systems, classical and quantum

Linear low energy excitations in fully-connected models of glasses

Silvio Franz[1], **Flavio Nicoletti**[2,*] **and Federico Ricci-Tersenghi**[2,3]

[1] LPTMS, UMR 8626, CNRS, Univ. Paris-Sud, Université Paris-Saclay, 91405 Orsay, France
[2] Dipartimento di Fisica, Università 'La Sapienza', P.le A. Moro 5, 00185, Rome, Italy
[3] INFN, Sezione di Roma1, CNR–Nanotec, Rome unit, P.le A. Moro 5, 00185, Rome, Italy
E-mail: flavio.nicoletti@uniroma1.it

Received 7 January 2022
Accepted for publication 31 March 2022
Published 12 May 2022

Online at stacks.iop.org/JSTAT/2022/053302
https://doi.org/10.1088/1742-5468/ac6518

Abstract. We study the linear excitations around typical energy minima of a mean-field disordered model with continuous degrees of freedom undergoing a random first order transition. Contrary to naive expectations, the spectra of linear excitations are ungapped and we find the presence of a pseudogap corresponding to localized excitations with arbitrary low excitation energy. Moving to deeper minima in the landscape, the excitations appear increasingly localized while their abundance decreases. Beside typical minima, there also exist rare ultra-stable minima, with an energy gap and no localised excitations.

Keywords: random matrix theory and extensions, spin glasses, energy landscapes, mode coupling theory

Contents

*Author to whom any correspondence should be addressed.

1742-5468/22/053302+31$33.00

1. Introduction

The nature of low energy excitations in glasses has attracted a lot of attention in the last few years [1–17]. Though glasses behave as solids, disorder induces low energy excitations—both of linear and non-linear—of very different nature to the ones of ordered solids. Remarkably, low energy excitations of glasses display a high degree of universality. In addition to usual phonons, in a variety of model glassy systems one finds the presence of ungapped and quasi-localized low energy excitations with density of states (DOS) behaving quadratically at low frequencies $\rho_{\rm QLS}(\omega) \sim A_4\omega^4$ [1–13]. The ω^4 behavior seems to be very general, independent of the system [9, 10, 18], preparation protocol [1] and even of the space dimension [5]. The coefficient A_4 on the other hand depends on the system and the preparation protocol. It appears that deeper states in the landscape, corresponding to better optimized glasses, have fewer and fewer low energy excitations, reflected by smaller and smaller values of A_4, and correspondingly, the excitations are more and more localized [12, 13]. This spectrum of localized modes was first rationalized through phenomenological theories [19, 20], while new predictions have recently enriched the picture. In [21–23], a mean-field model of unbounded soft spins inspired by [19] is exactly solved, finding a regime of parameters with a $D(\omega) \sim \omega^4$ spectrum.

In addition to typical ungapped minima, found by usual minimization protocols, it has been noticed in [24] that in some model glasses gapped mimima can be found through the use of smart minimization protocols that include particle swap [25, 26].

J. Stat. Mech. (2022) 053302

In such ultrastable minima the ω^4 spectrum is cut-off at low frequencies and localized excoriations are suppressed.

A theoretical comprehension based on microscopic models is however desirable. In such a context, long range spin glasses with continuous degrees of freedom provide a natural playground, the Hessian matrices turn out to be random matrices from classical ensembles and their spectral properties can be simply derived. Emblematic is the case of spherical disordered models [27, 28] and particles in high dimensional random landscapes where the Hessian belongs to either the Gaussian orthogonal ensemble (GOE)—for instance, the spherical p-spin models [27, 28] and related random landscape models [29, 30]—or Wishart ensembles [31] (perceptron model), with a constant shift on the diagonal that ensures that all eigenvalues are positive. In these cases, either the minima are gapped and the minimal excitations have a positive energy, or there is a square-root pseudo-gap, the spectrum behaves as $\rho(\lambda) \sim \sqrt{\lambda}$ and the non-linear (spin-glass) susceptibility, associated with the inverse second moment of λ, is divergent. In all these cases, eigenvectors are fully delocalized.

Recent work on soft-spin [21] and vectorial-spin [32] disordered models, however, has emphasized that even with long-range interactions non-trivial spectral pseudo-gaps can be present and some degree of localization is possible.

The aim of this paper is to extend our work on a spin-glass model with vectorial spins [32], where we showed that stable minima with a finite spin glass susceptibility, still have low energy quasi-localized excitations, resulting in a pseudo-gap in the spectral density. We are interested in studying glassy minima of long-range models with a glass transition of the one replica symmetry broken/random first order transition (1RSB/RFOT) kind [33]. These provide good mean-field models of the glass transition and have a finite complexity (configurational entropy) of stable glassy minima in a finite interval of low energy. We then consider a natural generalization of the p-spin model to vector spins [34–36], characterize the complexity of the energy minima, and study the spectral properties of the corresponding Hessian matrices. We find that typical stable minima have quasi-localized low energy excitations and no spectral gap. In addition, there are rare ultrastable minima where localized excitations are suppressed and the spectrum is gapped.

The structure of the paper is as follows: in section 2 we define the model and study its minima. In section 3 we study the complexity as a function of the energy. Then we study the spectral density in section 4 and the eigenvector statistics in section 5. In section 6 we study rare ultra-stable minima, where localized excitations are absent. Finally, in the discussion we draw our conclusions.

2. The model

We consider the following version of a p-spin model with vector spins. We have Nm-dimensional vector variables $\boldsymbol{S}_i$ with $i = 1, \ldots, N$ such that $|\boldsymbol{S}_i|^2 = \sum_{\alpha=1}^{m} (S_i^\alpha)^2 = 1$, interacting through a disordered Hamiltonian

$$\mathcal{H}[\boldsymbol{S}] = -\sum_p a_p \sum_{\boldsymbol{i},\boldsymbol{\alpha}} J_{i_1,\ldots,i_p}^{\alpha_1,\ldots,\alpha_p} S_{i_1}^{\alpha_1} \ldots S_{i_p}^{\alpha_p}, \tag{1}$$

J. Stat. Mech. (2022) 053302

where the couplings $J^{\alpha_1,\ldots,\alpha_p}_{i_1,\ldots,i_p}$ are Gaussian variables symmetric over all the indexes but otherwise independent, with zero mean and variance $\overline{(J^{\alpha_1,\ldots,\alpha_p}_{i_1,\ldots,i_p})^2} = \frac{p!}{2}N^{-(p-1)}$. The model generalizes to $O(m)$ spins the mixed p-spin model usually considered for Ising or spherical variables. It differs from the model considered by Panchenko in [36] by the fact that here all the spin components interact with each other, while in that model only components with the same label interact. This is a minor difference that does not affect the physics and it is only for notational simplicity that we choose the present version. As in the usual mixed p-spin model, an alternative formulation of the model is provided by defining the Hamiltonian as a Gaussian function with correlation function

$$\overline{\mathcal{H}[\boldsymbol{S}]\mathcal{H}[\boldsymbol{S}']} = N f(q(\boldsymbol{S}, \boldsymbol{S}')), \tag{2}$$

where $q(\boldsymbol{S}, \boldsymbol{S}')$ is the overlap

$$q(\boldsymbol{S}, \boldsymbol{S}') = \frac{1}{N}\sum_{i=1}^{N} \boldsymbol{S}_i \cdot \boldsymbol{S}'_i, \tag{3}$$

and the function f is

$$f(q) = \frac{1}{2}\sum_p a_p^2 q^p. \tag{4}$$

In this paper, we concentrate on the cases $m > 2$ and the pure monomial case where a single a_p with $p > 2$ is non-vanishing.

2.1. Minima of the Hamiltonian

The equations defining the minima of the model state in that each spin is aligned with its molecular field:

$$\partial\mathcal{H}[\boldsymbol{S}]/\partial S_i^\alpha + \mu_i S_i^\alpha \equiv \partial\mathcal{H}_i^\alpha + \mu_i S_i^\alpha = 0, \tag{5}$$

with

$$\mu_i = -\boldsymbol{S}_i \cdot \partial\mathcal{H}_i = |\partial\mathcal{H}_i|. \tag{6}$$

We are interested in low temperature linear excitations around the minima of energy E. These are ruled by the Hessian matrix. The Hessian, which we will implicitly think to be restricted to fluctuations orthogonal to each of the $\boldsymbol{S}_i$, can be written as

$$M_{ij}^{\alpha\beta} = \partial\partial\mathcal{H}_{ij}^{\alpha\beta} + \mu_i \delta_{ij}^{\alpha\beta}. \tag{7}$$

It is well known in these problems [28, 37] that independently of the value E of the energy, the matrix $\partial\partial\mathcal{H}$ can be considered as a GOE Wigner–Dyson matrix with random Gaussian i.i.d. elements with variance $\overline{(\partial\partial\mathcal{H}_{ij}^{\alpha\beta})^2} = f''(1)/N$. This can be seen from the explicit computation of the moments of the matrix elements and their mutual correlations [37]. The Hessian M is therefore a random matrix of the Porter–Rosenzweig (or deformed Wigner–Dyson) ensemble [38, 39] with elements μ_i on the diagonal.

J. Stat. Mech. (2022) 053302

Once knowing the μ_i, the statistical properties of eigenvalues and eigenvectors can be obtained by the 'local resolvent' elements $G_{ii}^{\alpha\alpha}(\lambda) = [(M - \lambda + i\epsilon)^{-1}]_{ii}^{\alpha\alpha}$, which verify the well-known equation

$$\sum_{\alpha} G_{ii}^{\alpha\alpha}(\lambda) = (m-1)\frac{1}{\mu_i - \lambda - f''(1)G(\lambda)}, \tag{8}$$

and $G(\lambda) = \sum_{i,\alpha} G_{ii}^{\alpha\alpha}(\lambda)/N$. Notice that for $\lambda = 0$, $G_{ii}^{\alpha\alpha}(0)$ is just the local susceptibility of the spin $\boldsymbol{S}_i$ to an applied field on site i. This should be a positive quantity for all i implying that $\mu_i > f''(1)G(0)$ for all i [40–43].

In order to study the stability properties of the minima we therefore need access to the distribution of the molecular fields μ_i. Before addressing this task, let us relate the true molecular field moduli μ_i to the 'cavity fields': that is the molecular fields computed when the ith variable is removed from the system.

2.2. A glimpse of the cavity method

At the basis of the application of the 'cavity method' [44], there is the hypothesis that the solutions to equation (5) are continuous upon removal or addition of a single spin. Suppose that a spin configuration $\boldsymbol{S}_j$ solves the complete set of equation (5), which includes the coupling with the spin i. Thanks to the fact that couplings are small, we can use linear response theory to relate $\boldsymbol{S}_j$ to the corresponding solution $\boldsymbol{S}_{j\to i}$ where the spin i is removed. We then write

$$S_j^{\alpha} = S_{j\to i}^{\alpha} + \sum_{\beta,\gamma} \chi_{jj}^{\alpha\beta} \partial\partial \mathcal{H}_{ji}^{\beta\gamma} S_i^{\gamma}, \tag{9}$$

which, introducing the cavity field $h_i = |\partial \mathcal{H}_i(\boldsymbol{S}_{\to i})|$ (the notation $\boldsymbol{S}_{\to i}$ means that the spin i is removed), allows us to conclude

$$\mu_i = h_i + f''(1)G_0 \quad \text{with } G_0 = \frac{1}{N}\sum_{\alpha j} \chi_{jj}^{\alpha\alpha}. \tag{10}$$

While equation (10) is generally valid for all minima, it does not inform us about the distribution of the cavity fields and its dependence on the energy level. We can obtain this information through the study of the complexity (configurational entropy) of typical minima with fixed energy E. Notice that equation (10) allows us to write a self-consistent equation for the resolvent from equation (8) that reads

$$G(\lambda) = (m-1)\left\langle \frac{1}{h - \lambda - f''(1)[G(\lambda) - G_0]} \right\rangle, \tag{11}$$

where the angular average is performed on the (still unknown) distribution of the cavity fields. Equation (11) implies that the susceptibility inside a state is related to the first inverse moment of the field distribution,

$$\chi = G_0 = G(0) = (m-1)\left\langle \frac{1}{h} \right\rangle, \tag{12}$$

J. Stat. Mech. (2022) 053302

while the spin glass susceptibility, $\chi_{\rm sg} = \frac{1}{N}\,\mathrm{Tr}\,M^{-2} = \frac{\partial G}{\partial \lambda}\big|_{\lambda=0}$ reads

$$\chi_{\rm sg} = \frac{1}{f''(1)}\frac{1-\Lambda}{\Lambda}, \tag{13}$$

$$\Lambda = 1 - (m-1)f''(1)\left\langle \frac{1}{h^2}\right\rangle, \tag{14}$$

leading to the stability condition $\Lambda > 0$. It can be shown that Λ is the 'replicon eigenvalue' appearing in the $T = 0$ replica formalism, and whose positivity is necessary for stability.

3. The complexity

According to the theory developed by Monasson in [45], the complexity of stable states can be computed through the replica method studying the replica symmetric free-energy for a non-vanishing number of replicas n. Compared with other existing methods, this has the advantage that with the same token one can study both thermodynamics and the properties of the metastable states. We need then to consider the average partition function of n replicas at temperature $T = 1/\beta$ where all the replicas have a mutual overlap q:

$$Z_n = \overline{\int \mathrm{d}\boldsymbol{S}\,\exp\left(-\beta\sum_{a=1}^{n}\mathcal{H}[\boldsymbol{S}_a]\right)\prod_{a,b}\delta(\boldsymbol{S}_a\cdot\boldsymbol{S}_b - Nq)}.$$

At the saddle point for q, the free-energy as a function of n, considered now as a positive real number, is related to the Legendre transform of the complexity of metastable states as a function of the free-energy g by

$$\mathcal{G}(n,T) = \frac{1}{N}\,\log\,Z_n = \Sigma(g,T) - \beta n g, \tag{15}$$

at the point where $\Sigma'(g) = \beta n$. In order to obtain the complexity of the energy minima, one should consider the limit $T \to 0$ and $n \to 0$ with $y = \beta n$ fixed: the result is $\mathcal{G}_0(y) = \Sigma(E) - yE$. A standard calculation that we reproduce in the appendix provides the expression of the replica symmetric finite n free-energy as follows:

J. Stat. Mech. (2022) 053302

$$\mathcal{G}(n,T) = \frac{n\beta^2}{2}\left[f(1) + (n-1)(f(q) - qf'(q)) - f'(q)\right] + \log\left[\frac{\int_0^\infty \mathrm{d}h\; h^{m-1} e^{-\frac{h^2}{2f'(q)}} Y(\beta h)^n}{\int_0^\infty \mathrm{d}h\; h^{m-1} e^{-\frac{h^2}{2f'(q)}}}\right], \tag{16}$$

$$Y(u) = (2\,\pi)^{m/2} \frac{I_{\frac{m-2}{2}}(u)}{u^{\frac{m-2}{2}}},$$

where $I_\nu(u)$ is the modified Bessel function of order ν. The overlap q between the replicas verifies the saddle point equation

$$q = \frac{\int_0^\infty \mathrm{d}h\; h^{m-1}\, \exp\left[-\frac{h^2}{2f'(q)}\right] Y(\beta h)^{n-2} Y'(\beta h)^2}{\int_0^\infty \mathrm{d}h\; h^{m-1}\, \exp\left[-\frac{h^2}{2f'(q)}\right] Y(\beta h)^n}. \tag{17}$$

From the replica free-energy one can also compute the 'replicon eigenvalue' Λ, whose positiveness is a necessary stability condition for the free-energy (16). Its expression is rather lengthy and we give it in appendix A.

Equation (17) has always a trivial $q = 0$ solution with vanishing complexity. Depending on the temperature, two $q > 0$ solutions can appear. The one with a small value of q is always unstable. The one with a larger q can be stable or unstable depending on the sign of Λ. From simple thermodynamics, we get the complexity of metastable states at temperature T as a function of the internal free-energy g:

$$g = -\frac{1}{\beta}\frac{\partial \mathcal{G}}{\partial n} \qquad \Sigma = -n^2 \frac{\partial \mathcal{G}/n}{\partial n}. \tag{18}$$

The complexity of equilibrium states at temperature T is obtained, as usual, considering the limit $n \to 1$ in the previous formulae. Different values of n, on the other hand, allow us to explore different families of metastable states, which have a collective vanishing weight at equilibrium. Notice that for fixed n and T, the present analysis gives us access to the distribution of the cavity field h. This distribution can be read directly from equation (16) and is written as:

$$P(h) = \frac{h^{m-1}\, \exp\left[-\frac{h^2}{2f'(q)}\right] Y[\beta h]^n}{\int_0^\infty \mathrm{d}h\; h^{m-1}\, \exp\left[-\frac{h^2}{2f'(q)}\right] Y[\beta h]^n}. \tag{19}$$

The behavior of metastable states is qualitatively similar to the case of the familiar spherical p-spin model and closely follows the RFOT pattern. The model is paramagnetic at high temperature, equation (17) has only the $q = 0$ solution and the Gibbs measure is concentrated on a single pure state. Below a dynamical transition temperature T_d ergodicity is broken. In the interval of temperatures $T_\mathrm{K}, T_\mathrm{d}$ an exponential number of mutually inaccessible metastable states dominates the equilibrium measure: in this situation equation (17) admits a stable solution with $q > 0$. Below T_K the number of

J. Stat. Mech. (2022) 053302

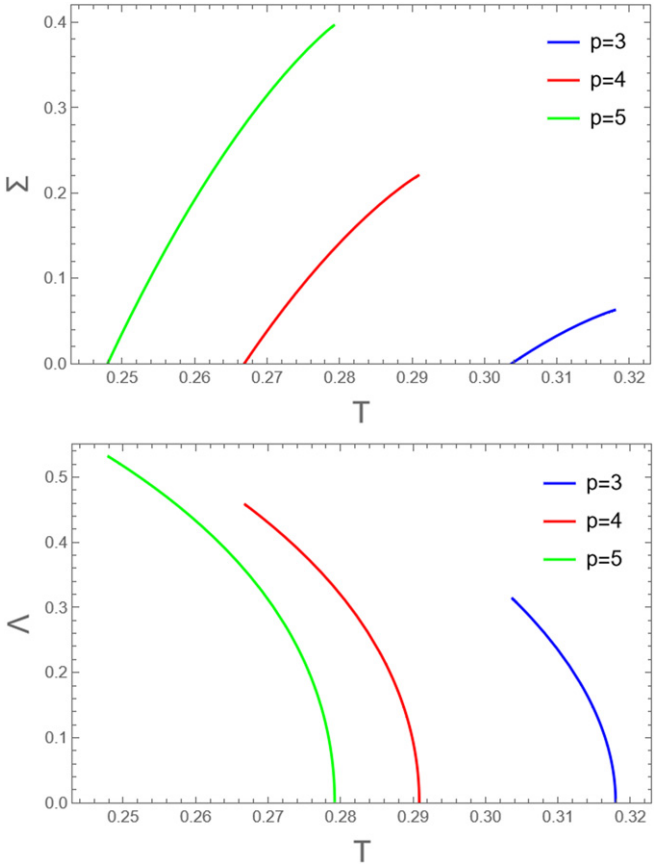

Figure 1. (Top) The equilibrium complexity Σ for the pure models with $m = 4$ and $p = 3$ (blue), $p = 4$ (red) and $p = 5$ (green). The complexity is different from zero in the interval of temperatures $(T_{\rm K}, T_{\rm d})$ and vanishes at $T_{\rm K}$. The value of the configurational entropy at $T_{\rm d}$ is $\Sigma_{\rm d} = 0.0627\,787$ $(p = 3)$, $\Sigma_{\rm d} = 0.220\,444$ $(p = 4)$, and $\Sigma_{\rm d} = 0.396\,359$ $(p = 5)$. (Bottom) The replicon eigenvalue Λ for the pure models with $m = 4$ and $p = 3$ (blue), $p = 4$ (red) and $p = 5$ (green). The replicon eigenvalue vanishes at $T_{\rm d}$ as $(T_{\rm d} - T)^{1/2}$.

states is sub-exponential, and the equilibrium measure concentrates on the lowest free-energy states. We notice that the replicon eigenvalue, which is vanishing for the states that dominate at $T_{\rm d}$, is positive at all temperatures below.

In figure 1, we show the equilibrium complexity and the replicon eigenvalue as a functions of T, for $m = 4$ and $p = 3, 4, 5$. Notice that Λ is positive for $T < T_{\rm d}$ and vanishes at $T_{\rm d}$ as $\Lambda \sim (T_{\rm d} - T)^{1/2}$.

The number of stable *energy* minima can be obtained performing the limit of $\mathcal{G}$ for $\beta \to \infty$, $n \to 0$, keeping the value $y = n\beta$ fixed. In this case, important simplifications occur and, observing that $Y(\beta h)^n \approx e^{yh}$, we get

$$\mathcal{G}_0(y) = \frac{1}{2} y^2 \left(f(1) - f'(1)\right) + \log \left[\frac{\int_0^\infty {\rm d}h\, h^{m-1} \exp\left(-\frac{h^2}{2f'(1)} + yh\right)}{\int_0^\infty {\rm d}h\, h^{m-1} \exp\left(-\frac{h^2}{2f'(1)}\right)} \right], \tag{20}$$

J. Stat. Mech. (2022) 053302

where the last term can be written in terms of confluent hypergeometric functions

$$\frac{\int_0^\infty \mathrm{d}h\, h^{m-1} e^{-\frac{h^2}{2f'(1)}+yh}}{\int_0^\infty \mathrm{d}h\, h^{m-1} e^{-\frac{h^2}{2f'(1)}}} = {}_1F_1\left(\frac{m}{2}\,;\frac{1}{2}\,;\frac{y^2 f'(1)}{2}\right) + \frac{\Gamma\left(\frac{m+1}{2}\right)}{\Gamma\left(\frac{m}{2}\right)} y\sqrt{2f'(1)}\,{}_1F_1\left(\frac{m+1}{2}\,;\frac{3}{2}\,;\frac{y^2 f'(1)}{2}\right). \tag{21}$$

The cavity field distribution in this limit takes the simple form of a reweighed chi distribution:

$$P(h) = p_0 h^{m-1} \exp\left[-\frac{h^2}{2f'(1)} + yh\right], \tag{22}$$

where p_0 is a normalization constant

$$p_0 = \frac{1}{\int_0^\infty \mathrm{d}h\, h^{m-1}\, e^{-\frac{h^2}{2f'(1)}+yh}} \equiv \frac{1}{Z_0}. \tag{23}$$

The replicon eigenvalue exactly takes the form in equation (13)

$$\Lambda = 1 - (m-1) f''(1) \left\langle \frac{1}{h^2} \right\rangle. \tag{24}$$

The study of Λ shows that the solution giving the complexity as a function of energy is stable around the ground state energy E_{gs}, and only becomes unstable at some higher values E_{mg} of the energy before disappearing at E_{last} [46]. In order to study the complexity beyond E_{mg} replica symmetry breaking should be included [47, 48], a task that we will not undertake in this paper. The complexity of the energy minima within the 1RSB approximation and the corresponding values of the replicon eigenvalue are shown in figure 2.

Comparing figures 1 and 2, we notice that $\Sigma_{\mathrm{d}} < \Sigma_{\mathrm{max}}$, where the number of energy minima is much larger than the maximum number of equilibrium states (those dominating the measure at T_{d}). This feature is at variance to what has been observed in the spherical pure p-spin model [49], where the lack of chaos in temperature preserves the number of states in the whole range of temperatures in the spin glass phase. Instead, it reminds what has been observed in the Ising p-spin model [50] and in the spherical mixed p-spin model [51], where the complexity of dominating states may change with the temperature.

4. The spectral density

We now have all the elements for studying the spectral density of the Hessian matrix in the energy minima from equations (11) and (22). Let us first make an argument allowing to estimate the spectrum in the region

$$\mathrm{Re}\; G(\lambda) - G_0 \ll 1, \qquad \mathrm{Im}\; G(\lambda) \ll 1. \tag{25}$$

J. Stat. Mech. (2022) 053302

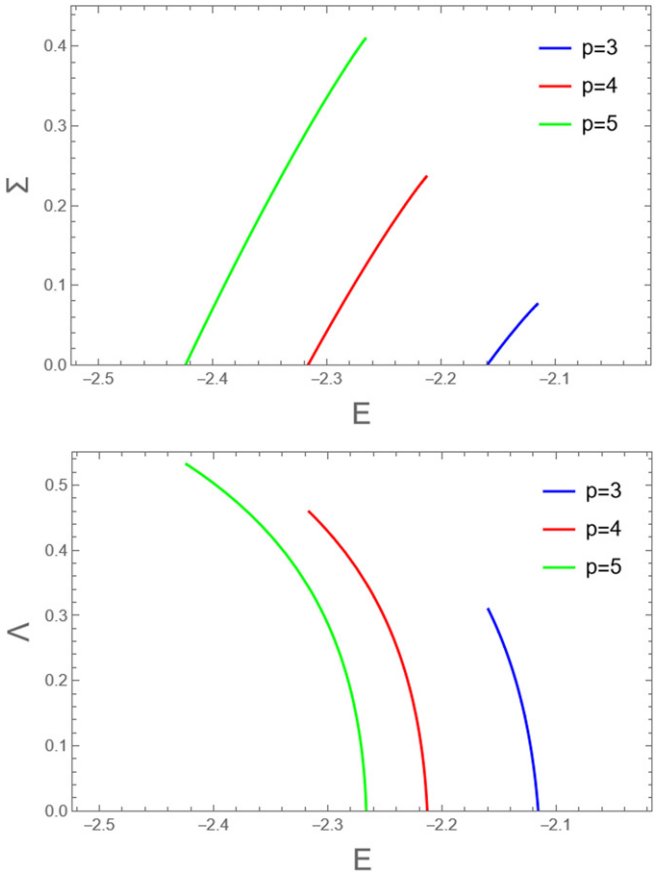

Figure 2. (Top) The complexity of the energy minima for the pure models with $m = 4$ and $p = 3$ (blue), $p = 4$ (red) and $p = 5$ (green). The maximum complexity is $\Sigma_{\max} = 0.0760\,961$ ($p = 3$), $\Sigma_{\max} = 0.236\,176$ ($p = 4$) and $\Sigma_{\max} = 0.409\,372$ ($p = 5$). The number of stable minima is considerably larger that the number of states at $T_{\rm d}$. (Bottom) The replicon eigenvalue in the energy minima for the pure models with $m = 4$ and $p = 3$ (blue), $p = 4$ (red) and $p = 5$ (green). Notice that here the replicon eigenvalue vanishes as $E_{\rm mg} - E$, although the slope is very large: we have $|\Lambda'(E_{\rm mg})| \simeq 23, 82, 212$ respectively for $p = 3, 4, 5$.

In order to make the argument simpler, let us assume that $m > 3$ so that $\left\langle \frac{1}{h^3} \right\rangle < \infty$. In that region, the leading contribution to the integral in equation (11) can be estimated expanding the denominator for small (but non vanishing) values of λ,

$$G(\lambda) \simeq (m-1)\left[\left\langle \frac{1}{h}\right\rangle + \left\langle \frac{1}{h^2}\right\rangle [\lambda + f''(1)(G(\lambda) - G_0)] + \left\langle \frac{1}{h^3}\right\rangle [\lambda + f''(1)(G(\lambda) - G_0)]^2\right], \tag{26}$$

which gives

J. Stat. Mech. (2022) 053302

$$\rho(\lambda) \propto \text{Im } G(\lambda) \propto \sqrt{\lambda - \lambda^*}, \tag{27}$$

$$\text{for } \lambda > \lambda^* \equiv \frac{\Lambda^2}{4(m-1)f''(1)\left\langle \frac{1}{h^3} \right\rangle}. \tag{28}$$

This expression would suggest the existence of a spectral gap $\lambda^* \sim \Lambda^2$ that vanishes only on marginal states where $\Lambda = 0$. However, the expansion in equation (26) is not valid for $\lambda \to 0$. In fact, any distribution of cavity fields extending its support to $h = 0$ is incompatible with a spectral gap, because close to $\lambda = 0$ we have $\text{Re}\, G(\lambda) - G_0 = \chi_{\text{sg}}\lambda$ and the real part of the denominator in equation (11) reads $h - \lambda/\Lambda$. That is, for all the minima but the marginal ones, if we had to admit $\text{Im}\, G = 0$, we would find that the integral in equation (11) is divergent. The only possible solution is to have $\rho(\lambda) > 0$ for any $\lambda > 0$, which is a pseudo-gap for $\lambda < \lambda^*$.

Detailed estimates presented in [32] allow us to conclude that, whenever the field distribution behaves as $P(h) \sim h^{m-1}$ close to the origin (which is the case here), in a stable minimum we have $\Lambda > 0$ and a spectral density behaving for small λ as

$$\rho(\lambda) = \frac{1}{\Lambda} P\left(\frac{\lambda}{\Lambda}\right) \approx A_m \lambda^{m-1} \quad A_m = \frac{p_0}{\Lambda^m}. \tag{29}$$

This is a pseudo-gap with a power law directly related to the cavity fields 'DOS' in the origin and is independent from the energy of the minimum. The prefactor A, conversely, depends on the energy and diverges for $\Lambda \to 0$. Notice that p_0 also depends on Λ implicitly, since it depends on y, which is a function of Λ. In figure 3, we show the dependence of the prefactor A_m with respect to the energy E, in the case of the pure p-spin with $m = 4$ and $p = 3, 4, 5$. We can see that this term has a strong dependence on the energy, varying by several order of magnitudes in the energy range of the 1RSB landscape. This feature is consistent with what observed for the computer glasses cited in the introduction of this work: the more the minimum is stable and low in energy, the smaller the prefactor is and, consequently, the more localised the excitations are (see discussion below).

As to the case $E = E_{\text{mg}}$ or $\Lambda = 0$, it was shown in [32] (and we convey the same calculation in appendix B) that the spectrum behaves as

$$\rho(\lambda) \approx \sqrt{\lambda} \quad m > 3, \tag{30}$$

$$\rho(\lambda) \approx \sqrt{\frac{\lambda}{|\log \lambda|}} \quad m = 3. \tag{31}$$

For finite Λ, the value $\lambda^* \propto \Lambda^2$, defined in equation (28), marks the crossover from the λ^{m-1} to the $\sqrt{\lambda}$ behaviors of the spectrum. In figure 4 we display the spectrum $\rho(\lambda)$ for $m = 4$, $p = 3$ and some values of y in the range $[y_{\text{mg}}, y_{\text{gs}}]$ where $y_{\text{mg}} = 1.42\,578$ and

J. Stat. Mech. (2022) 053302

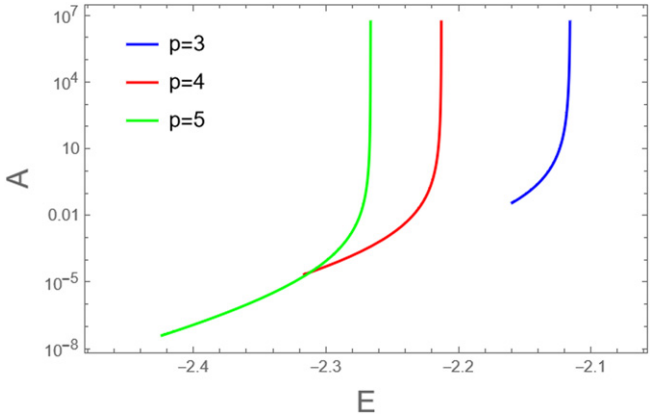

Figure 3. The prefactor A_4 of stable glassy minima is smaller for better optimized glasses. The dependence on the energy level E is very strong for high values of p: even far from $E_{\rm mg}$ this quantity varies by several orders of magnitude.

$y_{\rm gs} = 1.94\,874$. In the plot, we check the scaling laws in equations (29) and (30) and show the position of the crossover λ_* for each value of y.

5. The eigenvectors

The statistics of eigenvectors can be obtained from the study of the resolvent. It has been shown in [32] that the eigenvector components ψ_i^α corresponding to an eigenvalue λ in the bulk of the spectrum are Gaussian variables with a variance given by

$$\langle|\psi_i^\alpha|^2\rangle = \frac{m-1}{Nm|h_i + f''(1)(G_0 - G(\lambda)) - \lambda|^2}. \tag{32}$$

where the mean is performed at a fixed value of h_i [52]. Notice that the components α are not all independent, as $\boldsymbol{\psi}_i$ should be perpendicular to the spin $\boldsymbol{S}_i$ in the minimum under consideration. As a result, the inverse participation ratio, $\mathrm{IPR}(\lambda) = \sum_{i\alpha}\langle(v_i^\alpha)^4\rangle$, can be written as

$$\mathrm{IPR}(\lambda) = \frac{1}{N} i(\lambda) = \frac{3(m^2-1)}{N(m+2)} \int \mathrm{d}h \, \frac{P(h)}{|h + f''(1)(G_0 - G(\lambda)) - \lambda|^4}. \tag{33}$$

In the bulk, the IPR is of order $O(N^{-1})$ as it should for a dense matrix. However, close to the edge the eigenvectors are more and more localized. The quantity $i(\lambda)$ grows and diverges at the edges. In particular, at the lower edge one can see that

$$i(\lambda) \sim \Lambda^3 \left(\frac{\lambda}{\Lambda}\right)^{-2(m-1)}, \tag{34}$$

J. Stat. Mech. (2022) 053302

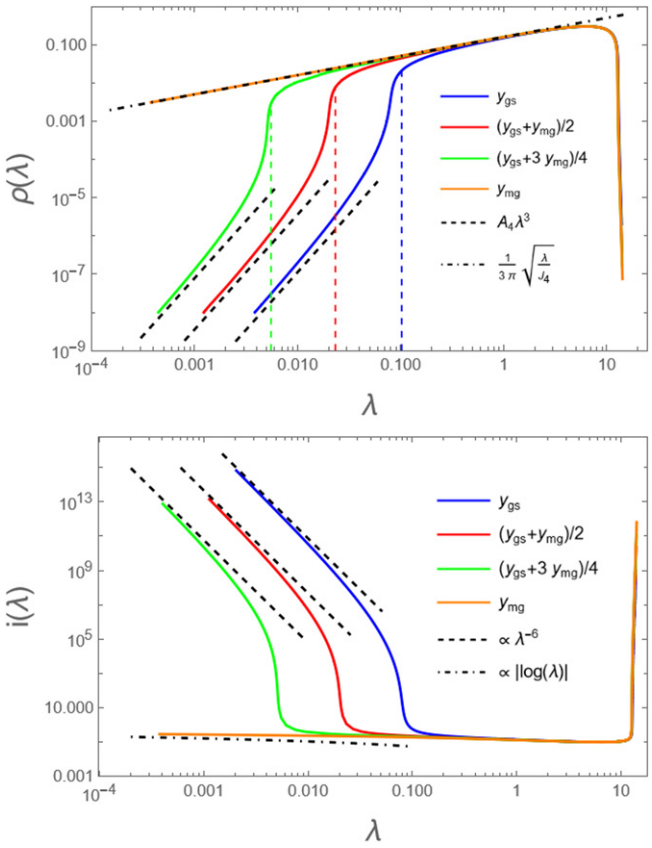

Figure 4. (Top) The spectrum of the Hessian in log–log scale for $m = 4$ and $p = 3$. The curves for $y < y_{\rm mg}$ cross-over from a λ^3 behavior to a $\sqrt{\lambda}$ behavior at λ_* marked by colored vertical dashed lines. In the bulk of the spectrum, the spectral density does not depend on y. (Bottom) The scaled bulk inverse participation ratio $i(\lambda)$ as a function of λ for $m = 4$ and $p = 3$ on a log–log scale. Notice the different behavior between the stable minima and the marginal one. The curve at $y_{\rm mg}$ diverges logarithmically, while the other curves behave as λ^{-6} for $\lambda \to 0$.

for stable minima and

$$i(\lambda) \propto \begin{cases} \sqrt{|\log \lambda|/\lambda} & m = 3 \\ |\log \lambda| & m = 4, \\ \text{const} & m > 4 \end{cases} \tag{35}$$

for the marginal ones. Notice that the minimum eigenvalues $\lambda_{\rm min}$ are of the order $\lambda_{\rm min} \sim \Lambda N^{-1/m}$ for stable minima and $\lambda_{\rm min} \sim N^{-2/3}$ for marginal ones. It is clear that for stable minima equation (34) cannot hold until $\lambda \sim \Lambda N^{-1/m}$, as this would imply an IPR of order $N^{1-2/m}$, which badly violates the bound IPR $\leqslant 1$. This suggest that the IPR could remain finite for the lower eigenvalues, as we will see is the case in the next section; we shall then refer to the IPR defined by equation (34) as *bulk* IPR. For marginally stable minima, the IPR of the smallest eigenvalue vanishes in the thermodynamic limit, meaning that the

J. Stat. Mech. (2022) 053302

softest modes are also delocalised; according to (35) the IPR of $\lambda_{\min} \sim N^{-2/3}$ goes to zero for $N \to \infty$ as $N^{-2/3}|\ln N|^{1/2}$ for $m = 3$, as $N^{-1}\ln(N)$ for $m = 4$ and as N^{-1} for $m \geqslant 5$. In figure 4, we show the rescaled bulk IPR, $i(\lambda)$, for $m = 4$, $p = 3$ and some values of y: stable minima have a rapidly diverging $i(\lambda) \sim \lambda^{-2(m-1)}$, whereas at the critical point the divergence is logarithmically slow, in accordance with equations (34) and (35). Notice that in the case of stable minima the IPRs of lowest eigenvalues should depart from the curves shown at a value $\lambda_* \simeq \Lambda^2$.

The necessity of the presence of localised excitations in the limit $\lambda \to 0$ can be understood in a more elegant way, by considering the normalisation condition of eigenvectors given by equation (32)

$$1 = \frac{1}{N}\sum_i \frac{f''(1)(m-1)}{|h_i + f''(1)[G_0 - G(\lambda)] - \lambda|^2}, \tag{36}$$

which is valid for all λ in the support of the spectral density. If one assumes that all sites provides a fine contribution to normalisation in the $\lambda \to 0$ limit, the normalisation condition then would be violated, since for $E < E_{\rm mg}$ the replicon is positive and equation (36) would imply $1 = (m-1)\frac{f''(1)}{N}\sum_i 1/h_i^2$, i.e. $\Lambda = 0$. In order to correctly satisfy the normalisation condition at the lower edge, it is necessary to have a condensate component, which yields a finite weight to normalisation in the thermodynamic limit:

$$1 \;=\; f''(1)(m-1)\left\langle \frac{1}{h^2} \right\rangle + |\vec{\psi}_C|^2. \tag{37}$$

This phenomenon, reminiscent of the Bose–Einstein condensation mechanism, is a very general feature of deformed Wigner matrices [53].

5.1. The spectral edge

It is interesting to study the statistics of the minimal eigenvalues and their relations to the low fields. This can be done using perturbation theory [54] around the diagonal matrix, which has the fields h_i as eigenvalues, which, without loss of generality we will suppose to be ordered in increasing order. The low eigenvalues of deep minima are associated with sites with small cavity field h_i with i finite for $N \to \infty$, which for deep minima are such that $h_i \sim N^{-1/m}$ and $h_{i+1} - h_i \sim N^{-1/m}$. In fact in correspondence with the lowest fields h_i, one finds multiplets of quasi-degenerate eigenvalues λ_i^a, $a = 1, \ldots, m-1$ with a typical splitting of order $N^{-1/2} \ll N^{-1/m}$. The eigenvalues can be computed in perturbation theory around the diagonal matrix $\mathrm{diag}(\mu_1, \ldots, \mu_N)$, which to the leading order gives [55].

$$\lambda_i^a = h_i + f''(1)G_0 + \frac{f''(1)}{N}\sum_{j\neq i}\frac{1}{h_i - h_j} \approx \Lambda h_i. \tag{38}$$

We obtain for the correspondent eigenvector

$$\psi^a_{k\alpha} = \sum_{\beta=1}^{m} \frac{\partial\partial\mathcal{H}^{\alpha\beta}_{ik} u^a_{k\beta}}{h_k} \quad k \neq i, \tag{39}$$

$$\psi^a_{i\alpha} = \sqrt{\Lambda} u^a_{i\alpha}, \tag{40}$$

where the $m-1$ vectors $\boldsymbol{u}^a_i$ are m-dimensional unit norm vectors orthogonal to $\boldsymbol{S}_i$ and to each other that at this level of accuracy in the perturbation theory are left unspecified. Notice that the eigenfunction ψ corresponding to the eigenvalue λ^a_i has finite components on the site i. The value of the condensate component is in agreement with equation (37).

6. Ultra-stable minima

Typical minima are ungapped due to localized excitations associated with sites with a small cavity field h_i. Since the number of minima is exponentially large, one can wonder if rare minima with a gap exist and what is their nature. In order to search for gapped minima, we need to include constraints in the computation of the complexity. Since low energy excitations are related to low cavity fields, it is natural to impose a hole in the distribution of the cavity field, $h_i > h_0 \forall\ i$ for some h_0, which we shall call a cavity gap.

The computation of the number of gapped minima is best performed using the Bray–Moore or Kac–Rice formalism [41, 56–58], computing

$$e^{\mathcal{G}_0(h_0)} = \overline{\int_{h_i>h_0} \mathrm{d}\boldsymbol{S}\,\mathrm{d}\boldsymbol{\mu}\; e^{-y\mathcal{H}} \prod_{i,\alpha} \delta\left(\partial\mathcal{H}^\alpha_i - \mu_i S^\alpha_i\right) \times \left|\det\left(\partial\partial\mathcal{H} - \mathrm{diag}(\mu)\right)\right|}. \tag{41}$$

Since the cavity fields are related to the physical fields $\mu_i = |\partial\mathcal{H}_i|$ by the equation $\mu_i = f''(1)\chi + h_i$, here we impose that $\mu_i > f''(1)\chi + h_0$. The determinant for fixed μ_i can be computed separately using self-averageness and the following representation of the determinant:

$$\begin{aligned}\overline{\left|\det\left(\partial\partial\mathcal{H} - \mathrm{diag}(\mu)\right)\right|} &= \overline{\det\left(-\partial\partial\mathcal{H} + \mathrm{diag}(\mu)\right)} \\ &= \left\{\overline{\int \frac{\mathrm{d}\boldsymbol{X}}{(2\pi)^{\frac{N(m-1)}{2}}} \exp\left[-\frac{1}{2}\boldsymbol{X}^{\mathrm{T}} \cdot \left(-\partial\partial\mathcal{H} + \mathrm{diag}(\mu)\right)\boldsymbol{X}\right]}\right\}^{-2}.\end{aligned}$$

After performing the average over the disorder and applying a Hubbard–Stratonovich transformation, one finds the final expression

$$\overline{\left|\det\left(\partial\partial\mathcal{H} - \mathrm{diag}(\mu)\right)\right|} = e^{\frac{Nf''(1)w^2}{2}} \prod_i \left[\mu_i - f''(1)w\right]^{m-1}, \tag{42}$$

J. Stat. Mech. (2022) 053302

where w is given by the solution of the saddle point equation

$$w = (m-1)\frac{1}{N}\sum_{i=1}^{N}\frac{1}{\mu_i - f''(1)w}. \tag{43}$$

Notice that by setting $\mu_i = h_i + f''(1)w$, this last equation can be rewritten for $N \to \infty$ as

$$w = (m-1)\int_{h_0}^{\infty} \mathrm{d}h\, \frac{P_{h_0}(h)}{h}, \tag{44}$$

so that w is just a 'cut' version of the $h_0 = 0$ susceptibility. In order to distinguish it from this last quantity, from now on we will call (44) $w \equiv \chi_{h_0}$. The remaining part can be averaged separately

$$\overline{\int \mathrm{d}\boldsymbol{S}\, e^{-y\mathcal{H}} \prod_{k,\alpha} \delta(\partial\mathcal{H}_k^{\alpha} + \mu_k S_k)} = \int \mathrm{d}\boldsymbol{S}\, \mathrm{d}\hat{\boldsymbol{S}}\, \exp -i\sum_{k=1}^{N} \mu_k \vec{S}_k \cdot \vec{\hat{S}}_k \times \overline{\exp\left[-\left(i\sum_{k,\alpha} \hat{S}_k^{\alpha}\frac{\partial}{\partial S_k^{\alpha}} + y\right)\mathcal{H}\right]},$$

where the $\hat{\boldsymbol{S}}$ are Lagrange multipliers introduced by the Fourier representation of the delta function. After the average over the disorder and one Hubbard–Stratonovich transformation, this last expression becomes

$$\left[\frac{1}{\Gamma(m/2) f'(1)^{m/2}}\right]^N \exp\left[\frac{1}{2}Ny^2 f(1) - N\frac{f''(1)u^2}{2} - \sum_i \frac{1}{2f'(1)}[y f'(1) + f''(1)u - \mu_i]^2\right], \tag{45}$$

with u given by the saddle point equation

$$u = \frac{1}{f'(1)N}\sum_{i=1}^{N}[\mu_i - y f'(1) - f''(1)u]. \tag{46}$$

Putting (42) and (45) together and defining the cavity fields $h_i = \mu_i - f''(1)\chi_{h_0}$, we obtain

J. Stat. Mech. (2022) 053302

$$\mathcal{G}_0(y\,;h_0) = \frac{y^2}{2}[f(1)-f'(1)] - \frac{f''(1)}{2f'(1)}(\chi_{h_0}-u)^2$$
$$- f''(1)y(u-\chi_{h_0}) - \frac{f''(1)}{2}(u^2-\chi_{h_0}^2) + \ln\, I(y\,;h_0). \tag{47}$$
$$I = \frac{\int_{h_0}^{\infty} \mathrm{d}h\, h^{m-1} e^{-\frac{h^2}{2f'(1)}+\frac{h}{f'(1)}[f''(1)(u-\chi_{h_0})+yf'(1)]}}{\int_0^{\infty} \mathrm{d}h\, h^{m-1} e^{-\frac{h^2}{2f'(1)}}}$$

Notice that the cavity field probability distribution

$$P_{h_0}(h) \;=\; \frac{\theta(h-h_0)}{Z(y\,;h_0)} h^{m-1} e^{-\frac{h^2}{2f'(1)}+\left[y+f''(1)\frac{(u-\chi_{h_0})}{f'(1)}\right]h}, \tag{48}$$

for $h_0 > 0$ has a finite cut on the lower edge, that is $P_{h_0}(h_0) > 0$, and is re-weighted in the exponential through the coefficient $y(h_0) = y + \frac{f''(1)(u-\chi_{h_0})}{f'(1)}$. Since $u - \chi_{h_0} > 0$ (see equation (49) below), $y(h_0) > y$ and therefore gapped minima are more stable than typical ungapped ones at the same value of y, and their energy is $E(y\,;h_0) = -\partial\mathcal{G}_0(y\,;h_0)/\partial y$. Different families of ultra-stable minima can be studied by varying y and h_0.

If the lower integration limit is $h_0 = 0$ it is easy to see by integration by part of (46) that $\chi_{h_0} = \chi = u$, and one gets back (21) and (19). However, this is not the case if $h_0 > 0$, indeed in such case one finds

$$u \;=\; \chi_{h_0} + P_{h_0}(h_0). \tag{49}$$

In fact, equation (43), which should be verified substituting the sum by the average over the cavity field distribution, cannot be interpreted as a saddle point condition for the expression in equation (47). The function u is indeed the actual static linear response function of the system inside an ultra-stable minimum: this quantity, for fixed y, is strictly lower than the response χ of gapless minima. A more detailed discussion of the response in ultra-stable minima can be found in appendix D.

In the remainder of this section we will discuss the spectral properties and the complexity of ultra-stable minima. The analytical details behind the formulae we are going to expose are provided in appendices C and E.

As we said, ultra-stable minima have a gapped spectrum, with a lower edge $\lambda_0 > 0$. It is found for small $\lambda - \lambda_0$ and for small h_0

$$\rho(\lambda) \propto \sqrt{\lambda-\lambda_0}$$
$$\lambda_0 \propto \begin{cases} \Lambda\, h_0, & y > y_{\mathrm{mg}} \\ h_0^{2(m-2)}, & m > 3, \quad y = y_{\mathrm{mg}} \\ h_0^2/|\ln\ h_0|, & m = 3, \quad y = y_{\mathrm{mg}}. \end{cases} \tag{50}$$

The linear dependence $\lambda_0 = \Lambda h_0$ valid for $y > y_{\mathrm{mg}}$ is easily interpreted. It tells that equation (38) relating small eigenvalues to small fields of typical minima is just cut-off here at the value h_0. The localized modes with $\lambda < \lambda_0$ are eliminated without much

J. Stat. Mech. (2022) 053302

other effect on the spectrum. For $y = y_{\rm mg}$ coherently, the induced spectral gap has a much weaker dependence on h_0.

The study of the IPR confirms that in ultrastable minima the most localized are cut-off. In the presence of a gap h_0, the integral appearing in the bulk IPR formula (33), remains finite in the limit $\lambda \to \lambda_0$. By expanding close to $\lambda = \lambda_0$, it is found at leading order

$$\begin{cases} i(\lambda) \sim h_0^{-2\,(m-1)}, & y > y_{\rm mg} \\ i(\lambda) \sim 1/h_0, & y = y_{\rm mg}, \quad m = 3 \\ i(\lambda) \sim \ln\, h_0, & y = y_{\rm mg}, \quad m = 4 \\ i(\lambda) \sim \text{const}, & y = y_{\rm mg}, \quad m \geqslant 5. \end{cases} \tag{51}$$

Details are provided in appendix E.

In the first panel of figure 5, we show the spectral density of gapless minima for $m = 4$, $p = 3$ and $y = (y_{\rm gs} + y_{\rm mg})/2$, comparing it with the spectral density of gapped minima with $h_0 = 0.15, 0.25, 0.8$: the square root behavior of the spectral edge of ultra-stable minima is confirmed. The spectral density has been computed by numerically solving the following equations

$$\begin{aligned} 1 &= (m-1) f''(1) \int_{h_0}^{\infty} {\rm d}h\, \frac{P_{h_0}(h)}{|h + x(\lambda)|^2} \\ \lambda &= f''(1)\chi_{h_0} - x_0 - f''(1)(m-1) \left\langle \frac{h + {\rm Re}\; x}{|h+x|^2} \right\rangle_{h_0}, \end{aligned} \tag{52}$$

where $x(\lambda) = f''(1)[\chi_{h_0} - G(\lambda)] - \lambda$. Equations (52) are respectively the imaginary and real part of the equivalent of equation (11) when the cavity field PDF is given by equation (48).

In the second panel of figure 5 we show, for the same m and p, the spectral gap as a function of the cavity gap for the values of $y > y_{\rm mg}$ reported in the legend of the plot, comparing the curves with $\Lambda(y)h_0$ in each case. The curves were obtained by solving numerically equation (52) fixing $\lambda = \lambda_0$. Finally, in the third panel of figure 5 we show the spectral gap for the case $y = y_{\rm mg}$ and $m = 3, 4, 5$, $p = 3$, showing the low cavity gap scaling of the λ_0, which is in good agreement with equation (50)

The energy and the complexity of the minima can be computed as usual from $\mathcal{G}_0(y\,; h_0) = -y\,E + \Sigma(E\,; h_0)$ and $E = -\partial \mathcal{G}_0(y\,; h_0)/\partial y$. For any value of y, Σ is a decreasing function of h_0: ultra-stable minima are exponentially small in number with respect to gapless ones. For a small cavity gap, the leading behavior is given by

$$\Sigma = \Sigma_0 - \left[\frac{1 + y\,\langle h \rangle_0}{m\, Z_0} \right] h_0^m + O(h_0^{m+1}), \tag{53}$$

where $\langle \cdot \rangle_0$ is the mean in the absence of gap and $Z_0 = 1/p_0$ (cfr with (23)). In figure 6 (top), we show the complexity as a function of the cavity gap h_0. The complexity is a decreasing function of h_0 that vanishes linearly at a value $h_0^{(\max)}(y)$. The value of $h_0^{(\max)}(y)$ goes to zero as y approaches its value on the ground state of the system. We have in

J. Stat. Mech. (2022) 053302

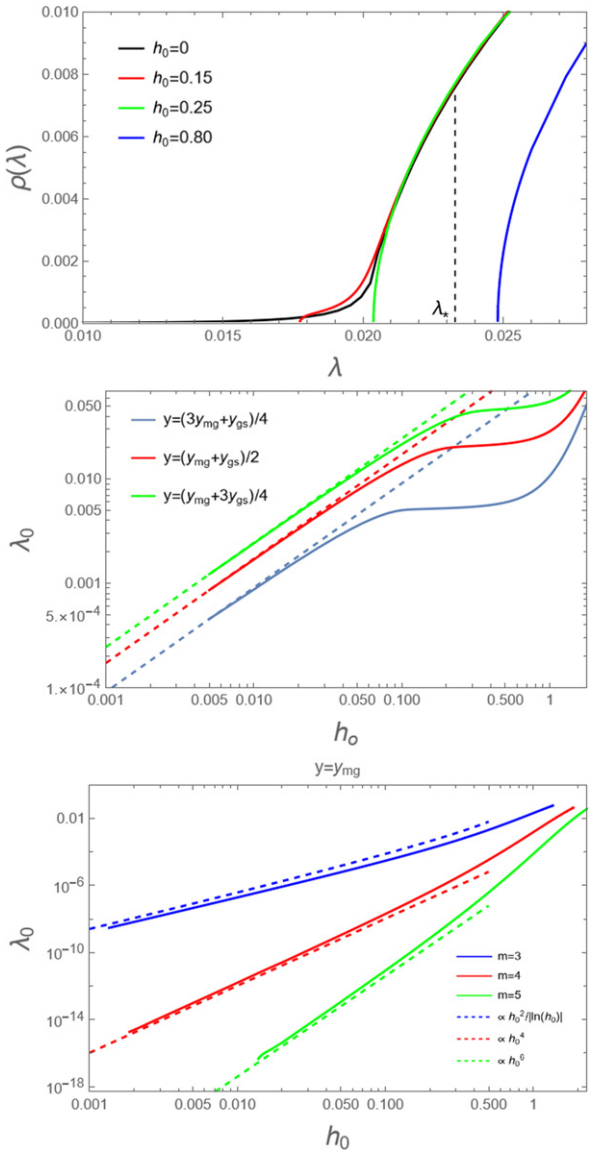

Figure 5. (Top) Spectral properties in the presence of a cavity gap h_0, for the $m = 4$ and $p = 3$ pure p-spin at $y = (y_{\rm gs} + y_{\rm mg})/2$. The spectral density of gapless minima is compared to that of minima with cavity gaps $h_0 = 0.15, 0.25, 0.8$. The dashed vertical line marks the position of the crossover λ_* in equation (28). (Center) The relation between the spectral gap and the cavity gap for the three values of $y \in [y_{\rm mg}, y_{\rm gs}]$, the dotted lines are $\Lambda(y)h_0$. (Bottom) The spectral gap at the critical point $y = y_{\rm mg}$ for $m = 3, 4, 5$: the scaling provided in appendix E is verified. Marginal minima develop extremely small gaps in a broad range of values of h_0.

fact $h_0^{(\max)}(y) \sim (y_{\rm gs} - y)^{1/m}$: in figure 6 (center), we check this behavior of the maximal cavity gap for the values of $m = 3, 4, 5$.

As a consistency check, to conclude this section, we show in figure 6 (bottom) that the energy $E(y;\ h_0)$ at the maximum cavity gap $h_0^{(\max)}(y)$ is always greater than the

J. Stat. Mech. (2022) 053302

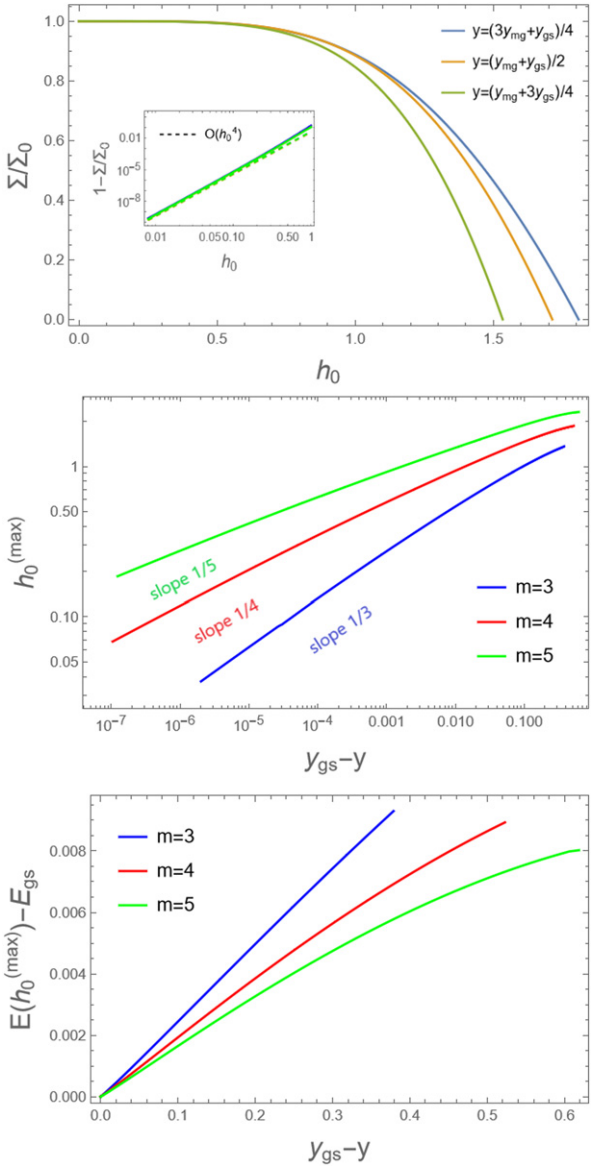

Figure 6. (Top) The normalised complexity Σ/Σ_0 for three values of $y \in [y_{\rm mg}, y_{\rm gs}]$ and $m = 4$: the complexity is a decreasing function of h_0, vanishing at a value $h_0^{(\max)}(y)$. In the inset, a plot in double log scale of $\Delta\Sigma = 1 - \Sigma/\Sigma_0$, which shows that for small cavity gap at leading order $\Delta\Sigma = O(h_0^4)$, in agreement with formula (53). (Center) The maximal cavity gap as a function of $y_{\rm gs} - y$ in double log scale, for $m = 3, 4, 5$: close to $y = y_{\rm gs}$, this quantity is singular as $(y_{\rm gs} - y)^{1/m}$. (Bottom) The difference between the energy at the maximal cavity gap and the ground state level as a function of $y = y_{\rm gs}$, for $m = 3, 4, 5$: there are no ultra-stable configurations down to the ground state.

ground state level $E_{\rm gs}$, for any $y < y_{\rm gs}$: there cannot be ultra-stable minima at the ground state level.

J. Stat. Mech. (2022) 053302

7. Discussion

In this work, we have studied the energy minima of a p-spin glass model with m-components vector spins interacting on a complete graph. The cases $m = 1$ and $m \to \infty$ reduce respectively to the familiar Ising and spherical p-spin models. Similarly to these cases, for $p > 2$ the model has a 1RSB-RFOT glassy phenomenology, with an exponential multitude of equilibrium states for temperatures between $T_{\rm K}$ and $T_{\rm d}$.

We have shown that generically, that is for any $1 < m < \infty$, these glassy models with continuous variables have stable glassy minima with quasi-localized low energy excitations. In this respect, spherical models, where stable minima are gapped and all excitations are fully extended, appear to be the exception rather than the rule.

We studied the complexity of the typical minima, which can be either 'stable', i.e. display a finite spin glass susceptibility, or marginal, with infinite spin glass susceptibility. In this paper, we concentrated on the stable minima and the lowest marginal ones that are described by replica symmetric theories.

Typical minima at each energy level are characterized by a cavity field distribution that extends down to zero. This in turn implies the existence of localized low energy excitations and the absence of a spectral gap. Different from what observed for models in physical space, the spectrum does not follow a universal ω^4 law. It is still a power law, but the power depends on m, the number of components of the vector spins. The prefactor of this power is function of the depth of the minima in the energy landscape, and it is smaller for lower energy. In addition to becoming less numerous, low energy excitations become more and more localized the deeper the minima in the landscape. Much less numerous than typical minima, rare ultrastable minima also exist where the small fields are absent, localized excitations are suppressed and spectra have a gap.

In this paper, we did not attempt a full characterization of marginal minima. The study of the complexity suggests the existence of marginally stable minima in some intervals of energy above the level $E_{\rm mg}$ that separates stable minima from marginal ones. These minima are described by replica symmetry breaking and could be the continuation of some high temperature states that undergo a Gardner transition [47, 48, 50, 56–61] at low temperature. Without much surprise, we can expect in these minima a divergent spin glass susceptibility, a square root spectral pseudogap and fully delocalized states.

A natural continuation of this work would be to investigate the spectral properties of low energy excitations of vector spin glass models with finite-connectivity, such as models on random graphs [62–68] or lattice models [15, 16]. This path would widen our knowledge of the nature of glassy excitations.

Appendix A. Computation of the Monasson free-energy

The computation of $\mathcal{G} = -\beta n f + \Sigma$ follows standard paths [45]. For completeness, we sketch here the main steps:

$$Z_n = e^{N\mathbf{G}} = \overline{\sum_{\boldsymbol{S}_a} e^{-\beta\sum_{a=1}^{n} H(\boldsymbol{S}_a)} \prod_{a<b}^{1,n} \delta(\boldsymbol{S}_a \cdot \boldsymbol{S}_b - qN)},$$

J. Stat. Mech. (2022) 053302

where $\sum_{\boldsymbol{S}}(\cdot) \equiv \prod_{k=1}^{N} \int \mathrm{d}\vec{S}_k\, \delta(S_k - 1)(\cdot)$. Performing the average and using $\overline{H(\boldsymbol{S})H(\boldsymbol{S}')} = Nf(q_{S,S'})$ one gets

$$e^{NG} = \exp\left\{\frac{N\beta^2}{2}[nf(1) + n(n-1)f(q)]\right\}\zeta(q)$$

$$\zeta(q) = \sum_{\boldsymbol{S}_a}\prod_{a<b}^{1,n}\delta(\boldsymbol{S}_a \cdot \boldsymbol{S}_b - q).$$

The quantity ζ after one Hubbard–Stratonovich transformation and the integration on spins becomes:

$$\begin{aligned}\zeta &= \mathrm{St}_{\hat{\mathrm{q}}}\left\{\exp\left[-N\frac{n(n-1)}{2}\hat{q}q + \frac{\hat{q}}{2}\sum_{a\neq b}\boldsymbol{S}^a \cdot \boldsymbol{S}^b\right]\right\} \\ &= \mathrm{St}_{\hat{\mathrm{q}}}\left\{\exp\left[-N\frac{n(n-1)}{2}\hat{q}q - N\frac{n}{2}\hat{q}\right]\left[\int D_{\hat{q}}\vec{h}\, Y(h)^n\right]^N\right\}.\end{aligned}$$

$$Y(h) = (2\,\pi)^{m/2}\frac{I_{\frac{m-2}{2}}(h)}{h^{\frac{m-2}{2}}}$$

$$\int D_{\hat{q}}\vec{h}\,(\cdot) \equiv \int \frac{\mathrm{d}\vec{h}}{(2\pi\hat{q})^{m/2}}\, e^{-\frac{h^2}{2q}}\,(\cdot).$$

Putting everything together and using the saddle point equation $\hat{q} = \beta^2 f'(q)$, we get (16). The physical overlap is found by extremizing $\mathcal{G}$ with respect to q and is given by equation (17): when $T > T_{\mathrm{d}}$, there is only the $q = 0$ solution, the system is in a paramagnetic phase with a unique equilibrium state and

$$\beta g_{\mathrm{para}} = \frac{\beta^2 f(1)}{2} + \log\, S_m. \tag{A1}$$

In the range $T_{\mathrm{K}} < T < T_{\mathrm{d}}$, (17) has a non-trivial solution, corresponding to a non-zero configurational entropy: configurations inside the same state have a non-zero overlap, whereas two configurations belonging to two different states have zero overlap. The stability of the non-trivial q is determined by the positiveness of the replicon eigenvalue of the replica free-energy Hessian:

$$\begin{aligned}\Lambda = 1 - \beta^2 f''(q)\Bigg\langle &\left\{\frac{m}{(\beta h)^2}\left[\frac{Y'(\beta h)}{Y(\beta h)}\right]^2\right. \\ &+ \left\{\frac{Y''(\beta h)}{Y(\beta h)} - \left[\frac{Y'(\beta h)}{Y(\beta h)}\right]^2 - \frac{Y'(\beta h)}{(\beta h)\,Y(\beta h)}\right\}^2 \\ &\left.+ \frac{2Y'(\beta h)}{(\beta h)\,Y(\beta h)} \times \left\{\frac{Y''(\beta h)}{Y(\beta h)} - \left[\frac{Y'(\beta h)}{Y(\beta h)}\right]^2 - \frac{Y'(\beta h)}{(\beta h)\,Y(\beta h)}\right\}\right\rangle.\end{aligned} \tag{A2}$$

J. Stat. Mech. (2022) 053302

The internal free-energies of TAP states and their complexity are obtained by equation (17) and they read

$$g = -\frac{\beta}{2}\left[f(1) + (2n-1)f(q) - (2n-1)qf'(q) - f'(q)\right] - \frac{1}{\beta}\langle \ln Y(\beta h)\rangle_n, \tag{A3}$$

$$\Sigma = -\frac{n^2\beta^2}{2}[f(q) - qf'(q)] + \ln \zeta - n\langle \ln Y(\beta h)\rangle_n, \tag{A4}$$

where ζ is defined in (16) and $\langle\cdot\rangle_n$ is an average with respect to (19).

Setting q equal to the correct physical value, one can explore different families of metastable states by varying n at fixed T in the range $[T_{\rm K}, T_{\rm d}]$, whereas the equilibrium values in the same interval are computed by setting $n = 1$. The equilibrium replicon vanishes at $T_{\rm d}$ as $(T_{\rm d} - T)^{1/2}$: at higher temperatures, the thermodynamic equilibrium is completely determined by the paramagnetic state $\boldsymbol{m} = 0$. The equilibrium complexity vanishes at $T_{\rm K}$ as $T - T_{\rm K}$: for lesser temperature, the equilibrium complexity remains zero, meaning that the Gibbs measure is concentrated on the lowest free-energy states.

The $T = 0$ limit is performed sending T and n to zero with $y = n/T$ fixed: the result given by equations (21) and (24) is retrieved by considering the asymptotic expansions of $Y(x)$, $Y'(x)/Y(x)$ and $Y''(x)/Y(x)$:

$$Y(x) \overset{x\to\infty}{\sim} \frac{(2\pi)^{m/2}\, e^x}{x^{m/2-1}} \left[\sqrt{\frac{1}{2\pi x}} + O\left(\frac{1}{x}\right)^{3/2}\right], \tag{A5}$$

$$\frac{Y'(x)}{Y(x)} \overset{x\to\infty}{\sim} 1 - \frac{m-1}{2\,x} + O\left(\frac{1}{x}\right)^2, \tag{A6}$$

$$\frac{Y''(x)}{Y(x)} \overset{x\to\infty}{\sim} 1 - \frac{m-1}{x} + O\left(\frac{1}{x}\right)^2. \tag{A7}$$

Appendix B. Spectrum of typical gapless minima

In this appendix, we will convey the analytical details concerning the spectrum of the energy minima: the analysis is very similar to the one presented in [32].

The PDF of the cavity fields moduli at $T = 0$, given by (22), extends in its support until zero field: as explained in section 4, in this situation the spectrum of the Hessian of $\mathcal{H}$ is necessary gapless. Defining the quantity $x(\lambda) \equiv f''(1)[G(0) - G(\lambda)] - \lambda$, the real

J. Stat. Mech. (2022) 053302

and imaginary parts of (11) satisfy

$$\text{Re } G(\lambda) \;=\; \left\langle \frac{h+\text{Re } x(\lambda)}{(h+\text{Re } x(\lambda))^2+\text{Im } x(\lambda)^2} \right\rangle, \tag{B1}$$

$$1 \;=\; f''(1)\left\langle \frac{1}{(h+\text{Re } x(\lambda))^2+\text{Im } x(\lambda)^2} \right\rangle. \tag{B2}$$

We now wish to consider the $\lambda \to 0$ expansion of these equations: to this purpose, we combine them and after some basic rearrangements we get

$$\begin{aligned} \lambda+\Lambda x \;&=\; -x^2 J - x|x|^2 I \\ J \;&=\; f''(1)(m-1)\left\langle \frac{1}{h|h+x|^2} \right\rangle \\ I \;&=\; f''(1)(m-1)\left\langle \frac{1}{h^2|h+x|^2} \right\rangle \end{aligned}, \tag{B3}$$

or equivalently

$$\begin{aligned} I|x|^2 &= -\Lambda - 2\,\text{Re } xJ \\ \lambda &= |x|^2 J \end{aligned}. \tag{B4}$$

When $\Lambda > 0$, the only way to compensate the vanishing of x for $\lambda \to 0$ in the first of (B4) is that I and J are divergent in such limit. For $\mathrm{d}G/\mathrm{d}\lambda(0) = \chi_{\text{SG}} \equiv \frac{1-\Lambda}{\Lambda}$, one has $\text{Re } x(\lambda) \simeq -\frac{\lambda}{\Lambda}$: if $|\text{Im}\, x(\lambda)| \ll |\text{Re}\, x(\lambda)|$, one can write $\frac{\text{Im } x}{(h+\text{Re } x)^2+\text{Im } x^2} \approx \pi\delta(h+\text{Re } x)$ and get

$$\begin{aligned} J &\approx \pi \frac{\tilde{P}(|\text{Re } x|)}{|\text{Re } x||\text{Im } x|} \\ I &\approx \pi \frac{\tilde{P}(|\text{Re } x|)}{|\text{Re } x|^2|\text{Im } x|} \end{aligned}, \tag{B5}$$

where $\tilde{P} = f''(1)(m-1)P$ and P is the cavity fields moduli PDF. Plugging these expansions into (B4), we finally get

$$\begin{aligned} \Lambda &= \pi \frac{\tilde{P}(|\text{Re } x|)}{|\text{Im } x|} \\ J &= \Lambda/|\text{Re } x| \\ \rho(\lambda) &= \frac{1}{m-1}|\text{Im } x|/\pi = f''(1)P(\lambda/\Lambda)/\Lambda \sim \lambda^{m-1}/\Lambda^m \end{aligned}, \tag{B6}$$

Equation (B6) are valid as long as $|\text{Re}\, x| \ll \Lambda$ and $|\text{Im}\, x| \ll |\text{Re}\, x|$, i.e. $\lambda/\Lambda \ll \lambda^{m-1}/\Lambda^m$ or $\lambda \ll \Lambda^{\frac{m-1}{m-2}}$. For $m > 3$, a stronger condition is found by considering only

J. Stat. Mech. (2022) 053302

$|\mathrm{Re}\, x| \ll \Lambda$: indeed, we find $\lambda \ll \Lambda^2$; this is equivalent to be at $\lambda \ll \lambda_*$, with $\lambda_* = O(\Lambda^2)$ defined in (27).

At the energy level $E = E_{\mathrm{mg}}$, we have $\Lambda = 0$: equations (B4) become

$$\begin{aligned} I|x|^2 &= -2\,\mathrm{Re}\; xJ \\ \lambda &= |x|^2 J. \end{aligned} \tag{B7}$$

Integrals I and J now, at variance with m, can be finite for $\lambda \to 0$. It is easy to see from these last equations that $|\mathrm{Re}\; x| = \frac{I}{2J^2}\lambda$ and $|\mathrm{Im}\; x| \equiv \pi\rho = \sqrt{\lambda/J_0} + O(\lambda)$, with $J_0 = f''(1)(m-1)\left\langle \frac{1}{h^3} \right\rangle$: when I and J are finite, it immediately follows $|\mathrm{Re}\, x| \ll |\mathrm{Im}\, x|$. Integrals I and J however are finite respectively only for $m > 4$ and $m > 3$. If $m = 4$, I has a logarithmic divergence and J is finite, $|\mathrm{Re}\; x| \sim \lambda|\ln\lambda| \ll |\mathrm{Im}\; x| \sim \sqrt{\lambda}$; at $m = 3$, if we assume again $|\mathrm{Re}\, x| \ll |\mathrm{Im}\, x|$, one finds $I \sim 1/|\mathrm{Im}\, x|$ and $|\mathrm{Re}\; x| \sim \sqrt{\lambda}|\ln\lambda|$, $|\mathrm{Im}\; x| \equiv \pi\rho \sim \sqrt{\lambda/|\ln\lambda|}$. Thus, for any $m \geqslant 3$ and $\Lambda = 0$

$$\begin{aligned} &|\mathrm{Re}\; x| \ll |\mathrm{Im}\; x| \\ &\rho \simeq \frac{1}{\pi\,(m-1)}\sqrt{\frac{\lambda}{J_0}}, \quad m > 3 \\ &\rho \simeq \frac{1}{2\pi}\sqrt{\frac{f''(1)\,Z_0\,\lambda}{2|\ln\,\lambda|}}, \quad m = 3. \end{aligned} \tag{B8}$$

Appendix C. Complexity of ultra-stable minima

In this appendix we show in greater detail all the computations concerning the complexity of the ultra-stable minima of the energy. First of all, we set $u - \chi_{h_0} = \Delta$, and rewrite (47)

$$\begin{aligned} \mathcal{G}_0(y\,;h_0) &= \frac{y^2}{2}[f(1) - f'(1)] - \frac{f''(1)}{2f'(1)}\Delta^2 \\ &\quad - yf''(1)\Delta - \frac{f''(1)}{2}\Delta(\Delta + 2\chi_{h_0}) + \ln\,\zeta(y\,;h_0) \\ \zeta_\Delta &= \frac{\int_{h_0}^{\infty}\mathrm{d}h\, h^{m-1}e^{-\frac{h^2}{2f'(1)} + \frac{h}{f'(1)}[f''(1)\Delta + yf'(1)]}}{\int_0^{\infty}\mathrm{d}h\, h^{m-1}e^{-\frac{h^2}{2f'(1)}}} \\ P_\Delta(h) &= \frac{\theta(h-h_0)}{Z(y\,;\Delta)}h^{m-1}e^{-\frac{h^2}{2f'(1)} + [yf'(1) + f''(1)\Delta]\frac{h}{f'(1)}}. \end{aligned} \tag{C1}$$

By combining equations (43) and (46) and approximating the sums with integrals, we find that Δ satisfies the self-consistent equation

$$\Delta = \frac{h_0^{m-1}\, e^{-\frac{h_0^2}{2f'(1)} + [y + f''(1)\Delta]h_0}}{\int_{h_0}^{\infty}\mathrm{d}h\, h^{m-1}\, e^{-\frac{h^2}{2f'(1)} + [y + f''(1)\Delta]h}} \equiv P_\Delta(h_0). \tag{C2}$$

In particular, for small h_0 one has ($Z_0(y) = 1/p_0$ defined in equation (23))

$$\Delta = \frac{h_0^{m-1}}{Z_0(y)}(1 + h_0 y) + O(h_0^{m+1}). \tag{C3}$$

The expression of $\Sigma(y;\ h_0)$ is obtained by applying the definition $\Sigma(y\,;h_0) = yE(y\,;h_0) + \mathcal{G}_0(y\,;h_0)$, and the full expression is

$$\begin{aligned}\Sigma(y\,;h_0) \;=\; & \Sigma(y\,;0) - \left[\frac{f''(1)^2}{f'(1)} + f''(1)\right] \\ & \times \left[\frac{1}{2} + \frac{y f'(1)(\langle h\rangle_\Delta - h_0)}{f'(1) + (\langle h\rangle_\Delta - h_0) f''(1)\Delta}\right]\Delta^2 \\ & - y[\chi_{h_0} + y f''(1)]\frac{f'(1)\,(\langle h\rangle_\Delta - h_0)}{f'(1) + (\langle h\rangle_\Delta - h_0) f''(1)\Delta}\Delta - \chi\Delta \\ & + \frac{y f'(1)[f''(1)(m-1) - \chi_{h_0}\langle h\rangle_\Delta]}{f'(1) + f''(1)(\langle h\rangle_\Delta - h_0)\Delta}\Delta \\ & - \frac{y f'(1)[\langle h\rangle_\Delta - \langle h\rangle_0] - \langle h\rangle_0(\langle h\rangle_\Delta - h_0)\Delta}{f'(1) + (\langle h\rangle_\Delta - h_0)\Delta} + \ln[\zeta_\Delta(y)/\zeta_0(y)],\end{aligned} \tag{C4}$$

where $\langle\cdot\rangle_\Delta$ is a mean according to P_Δ in (C1). This nasty expression can be simplified a lot by expanding for low cavity gap: by substituting (C3) one gets

$$\Sigma = \Sigma_0 - \left[\frac{1 + y\,\langle h\rangle_0}{m\,Z_0}\right] h_0^m + O(h_0^{m+1}). \tag{C5}$$

For $h_0 = O(1)$, Σ becomes proportional to $h_0^{(\max)}(y) - h_0$, thus vanishing at a certain maximal cavity gap. This last quantity is $O(1)$ far from $y_{\rm gs}$; as this point is approached, the maximal cavity gap is expected to vanish, since ultra-stable minima cannot be lower in energy than the ground state level. Taking $\Sigma = 0$ in (53), we can consider Σ_0 small and expand it linearly in $y_{\rm gs} - y$, getting

$$\left[\frac{1 + y\,\langle h\rangle_0}{m\,Z_0}\right](h_0^{\max})^m \simeq \frac{{\rm d}\Sigma_0}{{\rm d}y}(y_{\rm gs})(y_{\rm gs} - y)$$

$$h_0^{(\max)} \simeq A\,(y_{gs} - y)^{1/m}, \tag{C6}$$

$$A \;=\; \left[(m\,Z_0)\frac{\Sigma_0'\,(y)}{1 + y\langle h\rangle_0}\right]^{1/m}\Bigg| \, y = y_{\rm gs}, \tag{C7}$$

that is, a singularity approaching $y_{\rm gs}$.

Appendix D. Response function of ultra-stable minima

This appendix is devoted to the computation of the linear response function of the system when perturbed in an ultra-stable configuration at zero temperature: we show that the linear response function in this case is given by the order parameter u, which satisfies

$$u = \chi_{h_0} + P_\Delta(h_0).$$

Suppose to perturb the system with an external field $\vec{\epsilon}_i$ on each site: the static linear response function is given by

$$\mathcal{R} = \frac{1}{N}\sum_{i,\alpha} R_{ii}^{\alpha\alpha}, \tag{D1}$$

$$R_{ij}^{\alpha\beta} = \left.\frac{\partial\overline{\langle S_i^\alpha\rangle}}{\partial\epsilon_j^\beta}\right|_{\epsilon=0}, \tag{D2}$$

where off-diagonal terms of the response matrix are neglected since their disorder average is zero. Here, $\langle\cdot\rangle$ is an average according to Kac–Rice–Moore measure:

$$P_{\rm KRM} \propto e^{-y\mathcal{H}}\prod_{i,\alpha}\delta\left(\mathcal{H}_i^{\alpha'} - \mu_i S_i^\alpha\right)\left|\det\left(H'' - \mathrm{diag}(\mu)\right)\right|.$$

Then, one has for the response

$$\begin{aligned} R_{ii}^{\alpha\alpha} &= \langle(S_i^\alpha)^2\rangle - \langle S_i^\alpha\rangle^2 + i\langle S_i^\alpha\hat{S}_i^\alpha\rangle \\ \to \mathcal{R} &= \frac{1}{N}\sum_{k=1}^{N}\overline{\langle\vec{S}_k\cdot i\vec{\hat{S}}_k\rangle} \end{aligned}, \tag{D3}$$

where $\hat{S}_i^\alpha$ are Lagrange multipliers that ensures the $\boldsymbol{S}$ configuration is one of minimum of $\mathcal{H}$ (they are obtained from the Fourier representation of the delta function in (D3)). After performing similar passages to those explained in section 6, one finds for the relevant part of the integrals involved in the second equation of (D3)

$$\prod_l\int \mathrm{d}\vec{\mu}_l\int \mathrm{d}\vec{\hat{S}}_l\,(\vec{S}_k\cdot i\vec{\hat{S}}_k)e^{-\frac{f'(1)}{2}\hat{S}_l^2 - i[\mu_l - u - yf'(1)](\vec{S}_l\cdot i\vec{\hat{S}}_l)}$$

$$\propto -\left.\frac{\int \mathrm{d}\boldsymbol{\mu}\frac{\partial\, e^{-\sum_l\frac{c_l^2}{2f'(1)}}}{\partial c_k}}{\int \mathrm{d}\boldsymbol{\mu}\, e^{-\sum_l\frac{c_l^2}{2f'(1)}}}\right|_{c_l\equiv\mu_l-u-yf'(1)} = \frac{\overline{\mu} - u - yf'(1)}{f'(1)}.$$

J. Stat. Mech. (2022) 053302

The remainder of the integrals and factors cancel out with the normalization, and in the end we get

$$\mathcal{R} = \frac{1}{N}\sum_{k,\alpha}\overline{R_{kk}^{\alpha\alpha}} = \frac{1}{f'(1)}[\overline{\mu} - u - yf'(1)] \equiv u. \tag{D4}$$

To conclude this appendix, we show that u is always smaller than the susceptibility χ of the typical minimum configurations. From the definition of χ_{h_0} (equation (43))

$$\begin{aligned}\chi_{h_0} &= \chi - \frac{(m-1)\int_0^{h_0} \mathrm{d}h\, h^{m-2} e^{-\frac{h^2}{2f'(1)} + [yf'(1)+f''(1)\Delta]\frac{h}{f'(1)}}}{\int_{h_0}^{\infty} \mathrm{d}h\, h^{m-1} e^{-\frac{h^2}{2f'(1)} + [yf'(1)+f''(1)\Delta]\frac{h}{f'(1)}}} \\ &\equiv \chi - Q(h_0) < \chi,\end{aligned}$$

one finds

$$u = \chi - [Q(h_0) - P_\Delta(h_0)].$$

We notice that $Q(h_0) = (m-1)\int_0^{h_0} \mathrm{d}h\, \tilde{g}(h)$ and $P_\Delta(h_0) = h_0\tilde{g}(h_0)$, and thus we must determine if $(m-1)\int_0^{h_0} \mathrm{d}h\tilde{g}(h) - h_0\tilde{g}(h_0) > 0$; this inequality is indeed always verified for $m > 2$, since in this circumstance Q is a convex function: we conclude that $u < \chi$. In particular, for small h_0 it holds

$$u = \chi - \frac{1}{Z_0}[(m-1)(m-2) - 1]h_0^{m-1} + O(h_0^m). \tag{D5}$$

Appendix E. Spectrum of ultra-stable minima

When a cavity gap h_0 is present, one has a spectral gap $\lambda_0 > 0$ if the quantity $\mathrm{Re}\ x(\lambda) = f''(1)[\chi_{h_0} - G_R(\lambda)] - \lambda$ satisfies $|\mathrm{Re}\, x(\lambda_0)| < h_0$: in these circumstances, the spectral gap is determined by solving

$$\begin{aligned}1 &= (m-1)f''(1)\int_{h_0}^{\infty} \mathrm{d}h\, \frac{P_{h_0}(h)}{[h + \mathrm{Re}\ x(\lambda_0)]^2} \\ \lambda_0 &= (m-1)(\mathrm{Re}\ x(\lambda_0))^2 \int_{h_0}^{\infty} \mathrm{d}h\, \frac{P_{h_0}(h)}{h\,[h + \mathrm{Re}\ x(\lambda_0)]^2}.\end{aligned} \tag{E1}$$

We shall now consider the small h_0 limit of these last equations and the two cases $y > y_{\mathrm{mg}}$ and $y = y_{\mathrm{mg}}$. Let us begin with $y > y_{\mathrm{mg}}$: the first integral in (E1) is dominated by the values of h close to the cavity gap h_0; here $P_{h_0}(h_0) \sim h_0^{m-1}$, thus integrating in a small region $[h_0, ch_0]$ we get ($x_0 \equiv x(\lambda_0)$)

$$\begin{aligned}1 &\sim \frac{(1-1/c)(-x_0)^{(m-1)}}{Z_{h_0}(h_0 + x_0)} \\ x_0 &\sim -h_0 + \frac{(1-1/c)}{Z_{h_0}}|x_0|^{m-1}\end{aligned}, \tag{E2}$$

J. Stat. Mech. (2022) 053302

which ensures us that $|x_0| < h_0$. Then, rearranging the second of (E1)

$$\lambda_0 \;=\; f''(1)\chi_{h_0} - x_0 - f''(1)(m-1)\left\langle \frac{1}{h+x_0} \right\rangle_{h_0},$$

expanding $1/(h+x_0)$ in x_0/h and simplifying:

$$\lambda_0 \;=\; \Lambda|x_0| - f''(1)(m-1)x_0^2\left\langle \frac{1}{h^3} \right\rangle_{h_0} + O(x_0^3),$$

and plugging into this last equation equation (E2), it is found at leading order in h_0

$$\lambda_0 \;=\; \Lambda\, h_0 + O(h_0^2). \tag{E3}$$

We now consider the case $y = y_{\rm mg}$, i.e. $\Lambda = 0$. Here, one finds from the first of (E1)

$$\left\langle \frac{1}{h^2} \right\rangle_0 \;=\; \left\langle \frac{1}{(h+x_0)^2} \right\rangle_{h_0}, \tag{E4}$$

which after a few manipulations yields

$$|x_0| \;=\; \begin{cases} \dfrac{h_0^{m-2}}{2\,(m-2)\,Z_0\,\langle 1/h^3\rangle_0} + O(h_0^{m-1}), \;\; m>3 \\ \dfrac{h_0}{2\,|\ln\, h_0|} + O(h_0^2), \;\; m=3 \end{cases}. \tag{E5}$$

From the second part of (E1) expanding Λ_{h_0}, setting $\Lambda = 0$ and keeping terms up to order x_0^2, we find

$$\lambda_0 \;=\; \begin{cases} \left[\dfrac{f''(1)(m-1)}{4\,(m-2)^2\,Z_0^2\,\langle 1/h^3\rangle_0}\right] h_0^{2(m-2)} + O(h_0^{2(m-1)}), \;\; m>3 \\ \left[\dfrac{f''(1)}{2\;Z_0}\right] \dfrac{h_0^2}{|\ln\, h_0|} + O(h_0^4), \;\; m=3. \end{cases} \tag{E6}$$

We shall now consider the scaling of the spectral density and of the IPR close to λ_0. Equations (B3) are still valid if one replaces the ungapped $P_0(h)$ with the gapped one $P_{h_0}(h)$:

$$\begin{aligned} \lambda + \Lambda_{h_0} x \;&=\; -x^2\, J_{h_0} - x|x|^2\, I_{h_0} \\ J_{h_0}(\lambda) \;&=\; f''(1)(m-1)\left\langle \frac{1}{h|h+x|^2} \right\rangle_{h_0} \\ I_{h_0}(\lambda) \;&=\; f''(1)(m-1)\left\langle \frac{1}{h^2|h+x|^2} \right\rangle_{h_0}. \end{aligned}$$

Differently from the gapless case, here the integrals J_{h_0} and I_{h_0} are always finite in the limit $\lambda \to \lambda_0$, for any $y_{\rm mg} \leqslant y \leqslant y_{\rm gs}$: at $\lambda = \lambda_0$, it follows directly from $h_0 + x_0 > 0$. For $\lambda > \lambda_0$, one finds $h + x \simeq h + x_0 - \frac{m-3}{m-2}(\lambda - \lambda_0) + \mathrm{Im}\; x$, since $\mathrm{d}\mathrm{Re}\; x(\lambda_0)/\mathrm{d}\,\lambda = -\frac{m-3}{m-2}$; so the integrals are well defined if and only if $h_0 + x_0 + \mathrm{Im}\; x > \frac{m-3}{m-2}(\lambda - \lambda_0)$, so necessarily

J. Stat. Mech. (2022) 053302

$\mathrm{Im}\, x \gg O(\lambda - \lambda_0)$. In fact, one finds that the spectral density has a square root behavior close to the spectral edge:

$$\rho \simeq \sqrt{\frac{(1 - C_{h_0})(\lambda - \lambda_0)}{J_{h_0}}}, \tag{E7}$$

$$C_{h_0} \;=\; |x_0| \left(\frac{m-3}{m-2}\right) [2\, J_0 + |x_0|\, (\mathrm{d}J(x_0)/\mathrm{d}x)], \tag{E8}$$

$$J_{h_0} \;=\; f''(1)(m-1)\left\langle \frac{1}{h(h+x_0)^2} \right\rangle_{h_0}. \tag{E9}$$

As a consequence, the related lower edge eigenvectors of ultra-stable minima are found to be fully delocalised. Indeed, the IPR close to the spectral edge for $y > y_{\mathrm{mg}}$ behaves as

$$\begin{aligned} \mathrm{NPR}(\lambda) \propto \int_{h_0}^{\infty} \frac{\mathrm{d}h\, P_{h_0}(h)}{|h+x|^4} \;&=\; \int_{h_0}^{\infty} \frac{\mathrm{d}h\, P_{h_0}(h)}{(h+x_0)^4} \\ &+ O(\lambda - \lambda_0) \approx \frac{|x_0|^{m-1}}{3\, Z_0\, (h_0 + x_0)^3} \sim h_0^{-2\,(m-1)}. \end{aligned} \tag{E10}$$

At the critical point, we find by similar manipulations

$$\mathrm{NIPR}(\lambda_0) \sim \begin{cases} 1/h_0 & m = 3 \\ \ln\, h_0, & m = 4 \\ \mathrm{const}, & m \geqslant 5. \end{cases} \tag{E11}$$

References

[1] Lerner E, Düring G and Bouchbinder E 2016 *Phys. Rev. Lett.* **117** 035501
[2] Mizuno H, Shiba H and Ikeda A 2017 *Proc. Natl Acad. Sci.* **114** E9767
[3] Lerner E and Bouchbinder E 2017 *Phys. Rev.* E **96** 020104
[4] Shimada M, Mizuno H and Ikeda A 2018 *Phys. Rev.* E **97** 022609
[5] Kapteijns G, Bouchbinder E and Lerner E 2018 *Phys. Rev. Lett.* **121** 055501
[6] Angelani L, Paoluzzi M, Parisi G and Ruocco G 2018 *Proc. Natl Acad. Sci. USA* **115** 8700
[7] Wang L, Ninarello A, Guan P, Berthier L, Szamel G and Flenner E 2019 *Nat. Commun.* **10** 26
[8] Wang L, Berthier L, Flenner E, Guan P and Szamel G 2019 *Soft Matter* **15** 7018
[9] Richard D, González-López K, Kapteijns G, Pater R, Vaknin T, Bouchbinder E and Lerner E 2020 *Phys. Rev. Lett.* **125** 085502
[10] Bonfanti S, Guerra R, Mondal C, Procaccia I and Zapperi S 2020 *Phys. Rev. Lett.* **125** 085501
[11] Ji W, Popović M, de Geus T W J, Lerner E and Wyart M 2019 *Phys. Rev.* E **99** 023003
[12] Ji W, de Geus T W, Popović M, Agoritsas E and Wyart M 2020 *Phys. Rev.* E **102** 062110
[13] Ji W, de Geus T W, Agoritsas E and Wyart M 2021 arXiv:2106.13153
[14] Arceri F and Corwin E I 2020 *Phys. Rev. Lett.* **124** 238002
[15] Baity-Jesi M and Parisi G 2015 *Phys. Rev.* B **91** 134203
[16] Baity-Jesi M, Martín-Mayor V, Parisi G and Perez-Gaviro S 2015 *Phys. Rev. Lett.* **115** 267205
[17] Shimada M, Mizuno H, Berthier L and Ikeda A 2020 *Phys. Rev.* E **101** 052906

J. Stat. Mech. (2022) 053302

[18] Das P, Hentschel H G E, Lerner E and Procaccia I 2020 *Phys. Rev.* B **102** 014202
[19] Gurevich V, Parshin D and Schober H 2003 *Phys. Rev.* B **67** 094203
[20] Gurarie V and Chalker J T 2003 *Phys. Rev.* B **68** 134207
[21] Bouchbinder E, Lerner E, Rainone C, Urbani P and Zamponi F 2021 *Phys. Rev.* B **103** 174202
[22] Rainone C, Urbani P, Zamponi F, Lerner E and Bouchbinder E 2021 *SciPost Phys. Core* **4** 008
[23] Folena G and Urbani P 2021 arXiv:2106.16221
[24] Kapteijns G, Ji W, Brito C, Wyart M and Lerner E 2019 *Phys. Rev.* E **99** 012106
[25] Berthier L, Coslovich D, Ninarello A and Ozawa M 2016 *Phys. Rev. Lett.* **116** 238002
[26] Ninarello A, Berthier L and Coslovich D 2017 *Phys. Rev.* X **7** 021039
[27] Crisanti A and Sommers H-J 1992 *Z. Phys.* B **87** 341
[28] Cavagna A, Giardina I and Parisi G 1998 *Phys. Rev.* B **57** 11251
[29] Fyodorov Y V 2004 *Phys. Rev. Lett.* **92** 240601
[30] Fyodorov Y V and Le Doussal P 2018 *J. Phys. A: Math. Theor.* **51** 474002
[31] Franz S, Parisi G, Urbani P and Zamponi F 2015 *Proc. Natl Acad. Sci. USA* **112** 14539
[32] Franz S, Nicoletti F, Parisi G and Ricci-Tersenghi F 2022 *SciPost Phys.* **12** 016
[33] Parisi G, Urbani P and Zamponi F 2020 *Theory of Simple Glasses: Exact Solutions in Infinite Dimensions* (Cambridge: Cambridge University Press)
[34] Taucher T and Frankel N E 1992 *J. Stat. Phys.* **68** 925
[35] Taucher T and Frankel N E 1993 *J. Stat. Phys.* **71** 379
[36] Panchenko D 2018 *Ann. Probab.* **46** 865
[37] Auffinger A, Arous G B and Černý J 2013 *Commun. Pure Appl. Math.* **66** 165
[38] Rosenzweig N and Porter C E 1960 *Phys. Rev.* **120** 1698
[39] Brézin E and Hikami S 1998 *Phys. Rev.* E **57** 4140
[40] Palmer R G and Pond C M 1979 *J. Phys. F: Met. Phys.* **9** 1451
[41] Bray A J and Moore M A 1981 *J. Phys. C: Solid State Phys.* **14** 2629
[42] Bray A J and Moore M A 1982 *J. Phys. C: Solid State Phys.* **15** 2417
[43] Bray A J and Moore M A 1982 *J. Phys. C: Solid State Phys.* **15** L765
[44] Mézard M, Parisi G and Virasoro M A 1987 *Spin Glass Theory and beyond* (Singapore: World Scientific)
[45] Monasson R 1995 *Phys. Rev. Lett.* **75** 2847
[46] This is at variance with the Ising case, where all metastable states undergo a Gardner transition at a level specific temperature [47, 56, 60].
[47] Montanari A and Ricci-Tersenghi F 2003 *Eur. Phys. J.* B **33** 339
[48] Rizzo T 2013 *Phys. Rev.* E **88** 032135
[49] Castellani T and Cavagna A 2005 *J. Stat. Mech.* P05012
[50] Montanari A and Ricci-Tersenghi F 2004 *Phys. Rev.* B **70** 134406
[51] Folena G, Franz S and Ricci-Tersenghi F 2020 *Phys. Rev.* X **10** 031045
[52] For growing size N, the cavity fields become uncorrelated to the couplings, and we can therefore treat the off-diagonal elements and the diagonal ones of the Hessian as independent.
[53] Lee J O and Schnelli K 2016 *Probab. Theory Relat. Fields* **164** 165
[54] Landau L and Lifshitz E 1981 *Quantum Mechanics: Non-relativistic Theory, Course of Theoretical Physics* (Amsterdam: Elsevier)
[55] The same result can be obtained if one considers the condensation condition $|h_i + f''(1)[G(\lambda_i^a) - G_0] - \lambda_i^a| = O\ (N^{-1/2})$ (compare with formula (36)).
[56] Ros V, Arous G B, Biroli G and Cammarota C 2019 *Phys. Rev.* X **9** 011003
[57] Ros V, Biroli G and Cammarota C 2019 *Europhys. Lett.* **126** 20003
[58] Ros V, Biroli G and Cammarota C 2021 *SciPost* **10** 2
[59] Gardner E 1985 *Nucl. Phys.* B **257** 747
[60] Berthier L, Biroli G, Charbonneau P, Corwin E I, Franz S and Zamponi F 2019 *J. Chem. Phys.* **151** 010901
[61] Scalliet C, Berthier L and Zamponi F 2019 *Phys. Rev.* E **99** 012107
[62] Skantzos N S, Castillo I P and Hatchett J P 2005 *Phys. Rev.* E **72** 066127
[63] Coolen A C C, Skantzos N S, Castillo I P, Vicente C J P, Hatchett J P L, Wemmenhove B and Nikoletopoulos T 2005 *J. Phys. A: Math. Gen.* **38** 8289
[64] Marruzzo A and Leuzzi L 2015 *Phys. Rev.* B **91** 054201
[65] Lupo C and Ricci-Tersenghi F 2017 *Phys. Rev.* B **95** 054433
[66] Lupo C and Ricci-Tersenghi F 2018 *Phys. Rev.* B **97** 014414
[67] Lupo C, Parisi G and Ricci-Tersenghi F 2019 *J. Phys. A: Math. Theor.* **52** 284001
[68] Metz F L and Peron T 2021 arXiv:2110.11153

J. Stat. Mech. (2022) 053302